The human Golgi protein TMEM165 transports calcium and manganese in yeast and bacterial cells

Received for publication, December 9, 2019, and in revised form, February 10, 2020 Published, Papers in Press, February 11, 2020, DOI 10.1074/jbc.RA119.012249

Jiri Stribny[‡], Louise Thines[‡1], Antoine Deschamps[‡], Philippe Goffin[§], and Pierre Morsomme[‡2]

From the [‡]Louvain Institute of Biomolecular Science and Technology, Université Catholique de Louvain, B-1348 Louvain-la-Neuve, Belgium and the [§]Cellular and Molecular Microbiology Lab, Université Libre de Bruxelles, B-6041 Gosselies, Belgium

Edited by Mike Shipston

Cases of congenital disorders of glycosylation (CDG) have been associated with specific mutations within the gene encoding the human Golgi TMEM165 (transmembrane protein 165), belonging to UPF0016 (uncharacterized protein family 0016), a family of secondary ion transporters. To date, members of this family have been reported to be involved in calcium, manganese, and pH homeostases. Although it has been suggested that TMEM165 has cation transport activity, direct evidence for its Ca^{2+}- and Mn^{2+}-transporting activities is still lacking. Here, we functionally characterized human TMEM165 by heterologously expressing it in budding yeast (*Saccharomyces cerevisiae*) and in the bacterium *Lactococcus lactis*. Protein production in these two microbial hosts was enhanced by codon optimization and truncation of the putatively autoregulatory N terminus of TMEM165. We show that TMEM165 expression in a yeast strain devoid of Golgi Ca^{2+} and Mn^{2+} transporters abrogates Ca^{2+}- and Mn^{2+}-induced growth defects, excessive Mn^{2+} accumulation in the cell, and glycosylation defects. Using bacterial cells loaded with the fluorescent Fura-2 probe, we further obtained direct biochemical evidence that TMEM165 mediates Ca^{2+} and Mn^{2+} influxes. We also used the yeast and bacterial systems to evaluate the impact of four disease-causing missense mutations identified in individuals with TMEM165-associated CDG. We found that a mutation leading to a E108G substitution within the conserved UPF0016 family motif significantly reduces TMEM165 activity. These results indicate that TMEM165 can transport Ca^{2+} and Mn^{2+}, which are both required for proper protein glycosylation in cells. Our work also provides tools to better understand the pathogenicity of CDG-associated *TMEM165* mutations.

Post-translational modification of proteins by glycosylation is an essential biological process significantly influencing and modulating their structure and function. Genetically based abnormalities in protein glycosylation can result in congenital disorders of glycosylation (CDG),[3] a group of inherited diseases leading to wide variety of severe pathological symptoms. The group of CDGs has rapidly broadened over the last decade notably because of the development of advanced high-throughput sequencing techniques and consequent identification of responsible genes. This also involves a recent identification of a CDG subtype associated with specific mutations in the gene encoding TMEM165 (transmembrane protein 165) (1). TMEM165 belongs to a family of poorly characterized membrane proteins (UPF0016 and Pfam PF01169), which are highly conserved through evolution and widely distributed among a high number of prokaryotic and eukaryotic species. A specific signature of all the orthologous members is the presence of one or two copies of the highly conserved E*X*GD(K/R)(T/S) motif (2). We previously reported that TMEM165, as well as its *Saccharomyces cerevisiae* ortholog Gdt1p, localizes at the Golgi membrane (3). The exact physiological role of these proteins still remains to be fully deciphered. However, data obtained in recent studies gave several indications of their implication in calcium and manganese homeostasis. Namely, we reported that Gdt1p is required for high Ca^{2+} tolerance and proper Ca^{2+} response to salt stress (3). Regarding the manganese homeostasis, deletion of *GDT1* has been shown to lead to intracellular Mn^{2+} overaccumulation and to modulation of the activity of the Mn^{2+}-dependent enzyme Sod2p (4). The implication of Gdt1p, as well as of TMEM165, in manganese homeostasis is further supported by the fact that they are degraded by high external Mn^{2+} concentrations (5). Additionally in the presence of high Ca^{2+}, a lack of Gdt1p in yeast or TMEM165 in human cells was shown to result in protein glycosylation defects possibly because of an imbalanced Golgi-related homeostasis of calcium and/or manganese, two important elements for enzymes acting in glycosylation processes (5, 6). These glycosylation abnormalities can be in turn suppressed by Mn^{2+} supplementation (7). Based on these data, Gdt1p and TMEM165 were hypothesized to act as calcium/manganese transporters. Although Ca^{2+} and more recently Mn^{2+} transport capacity of Gdt1p was proven based on the use of fluorescent probes in Gdt1p-producing *Lactococcus lactis* (4, 8), no direct evidence of such transport capacity has been demonstrated for the clinically relevant TMEM165. In fact, development of such a direct approach would additionally prove useful for deeper investiga-

The work was supported by Fonds National de la Recherche Scientifique Grant PDR-T.0206.16. The authors declare that they have no conflicts of interest with the contents of this article.

This article contains Figs. S1 and S2.

[1] Research fellow at the Fonds pour le Formation à la Recherche dans l'Industrie et dans l'Agriculture.

[2] To whom correspondence should be addressed. E-mail: pierre.morsomme@uclouvain.be.

[3] The abbreviations used are: CDG, congenital disorder of glycosylation; ICP-AES, inductively coupled plasma atomic emission spectrometry; ER, endoplasmic reticulum.

tion of the functional impact of the specific missense mutations in TMEM165 identified in CDG patients.

Different mutations were detected in TMEM165 in the patients suffering from CDGs. One of these mutations (792 + 182G > A) causes the activation of a cryptic splice donor site that then leads to the WT transcript together with another transcript, resulting in a truncated and unstable protein (1). A second disease-causing mutation is found in the highly conserved ^{108}ELGDKT^{113} motif of TMEM165 (E108G) (9). The arginine at position 126 that belongs to a putative lysosomal-targeting motif ^{124}YNRL^{127} of TMEM165 was found mutated in two patients. One patient carried homozygous mutation R126H, whereas the other patient carried heterozygous missense mutation R126C and a missense mutation G304R (1). The effect of the identified missense mutations were studied mainly in terms of expression levels, subcellular localization of the protein, and glycosylation defects in mammalian cells (5, 10). However, if and how these mutations directly affect the activity of TMEM165 has yet to be examined. Because of difficulties in directly measuring ion fluxes in human cells, attempts have been carried out by heterologous expression of the mutated forms of TMEM165 in *S. cerevisiae* strain lacking *GDT1* and by subsequent phenotypic response to high Ca^{2+} concentrations. The full-length human TMEM165, however, could not complement the absence of Gdt1p, and only partial recovery was observed when truncating the 55 first N-terminal residues of the protein (3, 10). Because of these difficulties in producing an active form of TMEM165 in yeast, the phenotypic response of the mutations was therefore investigated only indirectly by introducing the corresponding changes at synonymous positions in the *S. cerevisiae GDT1* gene (6, 10, 11).

In this context, we primarily aimed to further improve the heterologous expression of the human TMEM165 in *S. cerevisiae* as well as in *L. lactis*. Indeed, these two heterologous systems constitute key tools to provide direct biochemical evidence for ion transport properties of TMEM165, as well as to further explore the impact of CDG-specific mutations on the transport activity. In the yeast strain with inactive Golgi-localized Ca^{2+}, Mn^{2+} transporters (Gdt1p and Pmr1p (12)) producing functional TMEM165, we first demonstrated an involvement of TMEM165 in resistance to high Ca^{2+} and Mn^{2+} concentrations, as well as in cellular manganese accumulation, thereby strengthening the fact that TMEM165 would transport calcium and manganese. On the other hand, in *L. lactis* cells producing TMEM165, we were able to directly show TMEM165-dependent calcium and manganese influx. We finally used these two systems to study the impact of disease-causing mutations on the transport activity of the human protein. Taken together, these data provide direct evidence of calcium and manganese transport by TMEM165, thereby opening up new avenues for a better understanding of the related disorders of glycosylation.

Results

Optimization of the heterologous expression of TMEM165 in yeast

Gdt1p is required for calcium homeostasis in yeast because a *gdt1*Δ strain is sensitive to high external Ca^{2+} concentration (3). This phenotype is exacerbated in a strain deleted for the Golgi-localized Ca^{2+}/Mn^{2+}-ATPase *PMR1* (3, 8). Also, it has been shown that a truncated version of TMEM165 partially restores the growth of *gdt1*Δ strain under high Ca^{2+} concentration. The N-terminal extension of TMEM165 is not present in Gdt1p and has been hypothesized to act as a nonconserved autoregulatory domain (3). To improve the expression and activity of TMEM165 in yeast, we have constructed three codon-optimized versions of TMEM165: a full-length version (TMEM165), a version truncated of the first 55 amino acids ($^{\Delta55}$TMEM165), and a version truncated of the first 78 amino acids ($^{\Delta78}$TMEM165) (Fig. S1). The $^{\Delta78}$TMEM165 version is equivalent to the yeast $^{\Delta23}$Gdt1p in which the putative signal sequence has been removed. As shown in Fig. 1*A*, the codon optimization significantly improved the heterologous production of the three TMEM165 versions in *S. cerevisiae* *gdt1*Δ*pmr1*Δ strain.

Fig. 1*B* shows that the nonoptimized full-length TMEM165 was not able to complement the growth defect of the *gdt1*Δ*pmr1*Δ in the presence of 400 mM Ca^{2+}, whereas the nonoptimized $^{\Delta55}$TMEM165 slightly decreased the Ca^{2+} sensitivity. This Ca^{2+} sensitivity was, on the other hand, fully suppressed by the expression of the codon-optimized versions of TMEM165. Strikingly, the expression of $^{\Delta78}$TMEM165 confers higher tolerance when compared with the strains expressing the other TMEM165 variants as well as *GDT1*. Because the truncated versions are produced at approximately the same level, this better complementation is likely due to the differential truncation. This phenotype is consistent with the previously discussed possibility that the nonconserved N-terminal part of TMEM165 acts as an autoregulatory domain (3).

Expression of TMEM165 in yeast modulates its Mn^{2+} homeostasis

In addition to calcium homeostasis, Gdt1p and TMEM165 were recently proposed to play an important role in the regulation of Golgi Mn^{2+} homeostasis (4, 7). Additionally, it was previously shown that deletion of *GDT1* confers an extrasensitivity toward Mn^{2+} in the *pmr1*Δ background. The expression of the full-length TMEM165 and the $^{\Delta55}$TMEM165 variants in the *gdt1*Δ*pmr1*Δ strain did not restore the tolerance to high Mn^{2+} because the growth was similar to that of the control strain harboring an empty vector. On the contrary, and just as observed in Ca^{2+}-related phenotypic assay, the sensitivity level of the *gdt1*Δ*pmr1*Δ strain to high Mn^{2+} was diminished by expression of the truncated $^{\Delta78}$TMEM165 (Fig. 2*A*). To provide further evidence of the involvement of TMEM165 in Mn^{2+} homeostasis, the total Mn^{2+} levels of the WT strain and of *gdt1*Δ*pmr1*Δ carrying different TMEM165 forms were evaluated using inductively coupled plasma atomic emission spectrometry (ICP-AES) (Fig. 2*B*). Consistent to our recently reported data (4), the cellular Mn^{2+} content of the *gdt1*Δ*pmr1*Δ strain was ~30-fold higher when compared with the WT. As already indicated by the growth assay, the cellular Mn^{2+} content of *gdt1*Δ*pmr1*Δ was significantly decreased when expressing $^{\Delta78}$TMEM165. It displayed even lower Mn^{2+} content than *gdt1*Δ*pmr1*Δ expressing *GDT1*, suggesting that $^{\Delta78}$TMEM165 would be more active than Gdt1p, as also indicated by the growth test. Interestingly, whereas the growth of the *gdt1*Δ*pmr1*Δ mutant expressing TMEM165 or the $^{\Delta55}$TMEM165

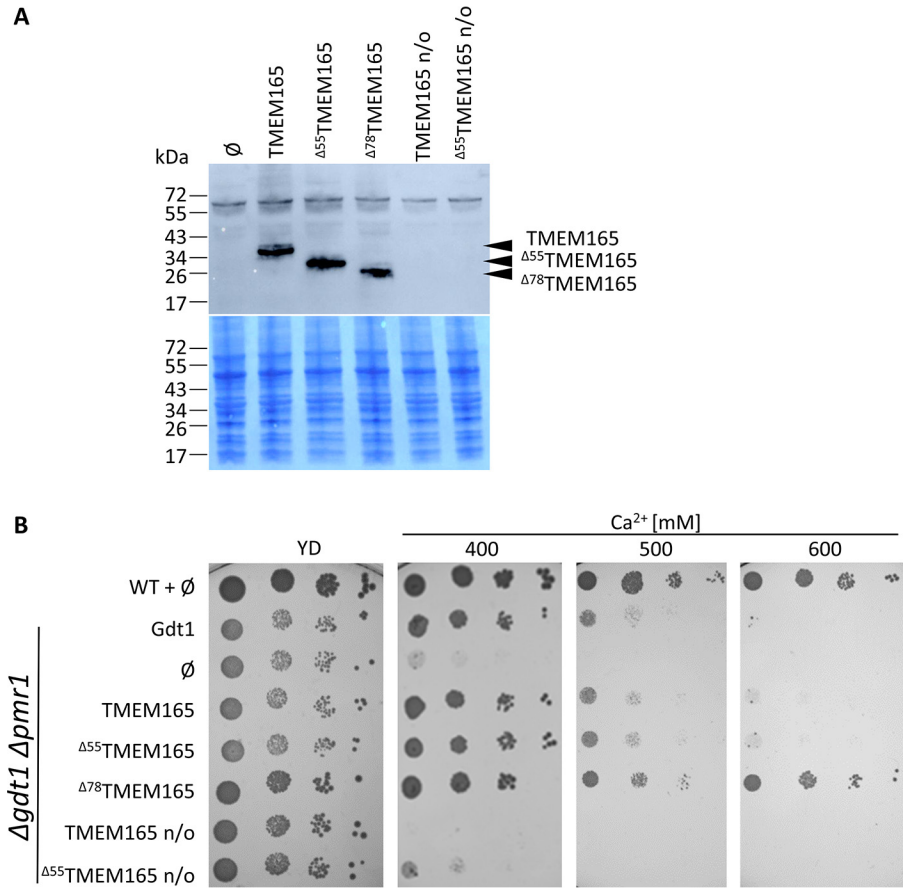

Figure 1. *A*, production of the different TMEM165 versions in *gdt1*Δ*pmr1*Δ strain. Total protein extracts of cells grown in MD-U medium to an A_{600} of 3 were analyzed by Western blotting with antibodies directed against TMEM165. ∅, *gdt1*Δ*pmr1*Δ with the empty pRS416 vector. Coomassie Blue–stained polyvinylidene fluoride membranes were used as loading control. *B*, growth of the WT strain and *gdt1*Δ*pmr1*Δ in MD-U medium supplemented or not with $CaCl_2$. The *gdt1*Δ*pmr1*Δ strain expressed *GDT1*, TMEM165, or its different truncated versions under the control of the constitutive *TPI1* promoter. *n/o*, codon nonoptimized versions of TMEM165. The cells were precultured overnight in MD-U medium. The cultures were subsequently adjusted to an A_{600} of 0.3, and serial 10-fold diluted cultures were dropped on MD-U solid medium containing indicated concentrations of $CaCl_2$. The plates were incubated 3 days at 28 °C.

was similar to the negative control (with empty vector) when exposed to high Mn^{2+}, the total Mn^{2+} content of *gdt1*Δ*pmr1*Δ expressing either of the two TMEM165 forms was significantly lower than the negative control and reached levels similar to the strain expressing *GDT1*. This indicates that although not capable of suppressing the sensitivity of *gdt1*Δ*pmr1*Δ to high Mn^{2+}, the full-length TMEM165 and the $^{\Delta 55}$TMEM165 are still functionally efficient to complement the absence of *GDT1* in terms of the Mn^{2+} content regulation.

Truncated TMEM165 mediates Ca^{2+} and Mn^{2+} influx in L. lactis

To unambiguously demonstrate the transport activity of TMEM165, we performed an *in vivo* functional transport assay in the *L. lactis* DML1 strain loaded with the fluorescent Ca^{2+}/Mn^{2+}-sensitive Fura-2 probe. Using this strategy, we have previously demonstrated Ca^{2+} and Mn^{2+} transport activity of Gdt1p (4, 8). As mentioned above, the combination of the codon optimization and truncation of the nonconserved N-terminal sequence improved the heterologous expression and functional complementation of TMEM165 in *S. cerevisiae*. We therefore selected the two truncated variants of TMEM165 and applied a codon optimization specific for heterologous expression in bacteria (Fig. S2). We then verified that these two forms are indeed well-produced in the selected bacterial host (Fig. 3*A*). The *L. lactis* cells expressing $^{\Delta 55}$TMEM165 or $^{\Delta 78}$TMEM165 or containing the empty vector were loaded with the Fura-2 probe. The changes in fluorescence intensity monitored over time correspond to variation of intracellular free cation (Ca^{2+}/Mn^{2+}) concentration, reflecting Ca^{2+} or Mn^{2+} transport (Fig. 3*B*). Upon addition of $CaCl_2$ in the external medium, the cells expressing the truncated TMEM165 variants exhibited a strong increase of the emission of fluorescence at 510 nm after excitation at 340 *versus* 380 nm (ratio 340/380), reflecting Ca^{2+} influx, whereas almost no increase was detected in the control strain harboring the empty plasmid. The Mn^{2+} transport assay takes advantage of the fact that manganese quenches Fura-2– emitted fluorescence, which, when excited at 360 nm (the Fura-2 isosbestic point), is independent of the Ca^{2+} concentration (4). Similarly as for Ca^{2+} transport, the cells expressing the two TMEM165 variants exhibited significantly more pronounced fluorescence quenching after the addition of $MnCl_2$ when compared with the negative control. Although the slight signal decrease observed for the negative control might reflect transport of Mn^{2+} by *L. lactis* endogenous transporters, the stronger quenching observed for the clones producing either of the TMEM165 indicates that they me-

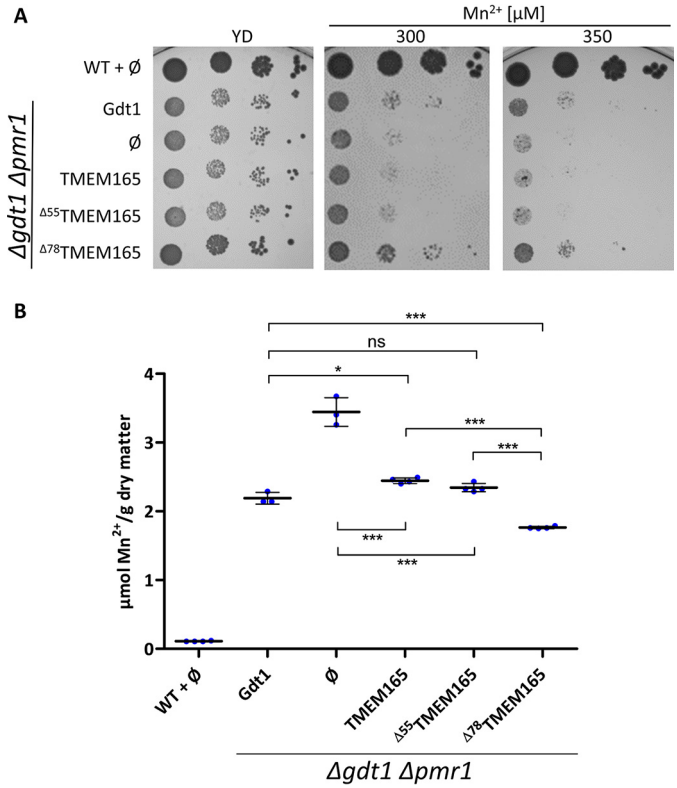

Figure 2. A, Growth of the WT strain and *gdt1Δpmr1Δ* in MD-U supplemented or not with $MnCl_2$. The *gdt1Δpmr1Δ* strain expressed *GDT1*, TMEM165, or its different truncated versions under the control of the constitutive *TPI1* promoter. ∅, *gdt1Δpmr1Δ* with the empty pRS416 vector. The cells were treated as described in Fig. 1*B*. *B*, cellular Mn^{2+} content of the WT and *gdt1Δpmr1Δ* expressing *GDT1*, TMEM165, or its different truncated versions under the control of the constitutive *TPI1* promoter. The strains were grown in MD-U medium to an A_{600} of 3, and the cellular Mn^{2+} content was measured by ICP-AES. The data are shown as means ± S.D. ($n = 4$). *, $p < 0.05$; ***, $p < 0.001$ (one-way analysis of variance with Bonferroni post hoc test). *ns*, not significant.

diate Mn^{2+} influx in *L. lactis*. Strikingly, the cells expressing $^{\Delta 78}$TMEM165 exhibited markedly more pronounced 340/380 increase and more intense fluorescence quenching than the cells with $^{\Delta 55}$TMEM165, reflecting better capability of the shorter TMEM165 version to mediate Ca^{2+} and Mn^{2+} transport in *L. lactis*. This observation supports the above described data obtained in *S. cerevisiae*–related assays. Given this higher activity, $^{\Delta 78}$TMEM165 was selected to determine its affinity for Ca^{2+} and Mn^{2+} and to further investigate whether the CDG-linked mutations affect the transport activity.

The apparent K_m for Ca^{2+} and Mn^{2+} were determined by *in vivo* transport measurements in *L. lactis* at a range of concentrations of $CaCl_2$ and $MnCl_2$ (2.5–200 μM $CaCl_2$ and 10–400 μM $MnCl_2$). The analysis, which exhibited typical Michaelis–Menten saturation kinetics (Fig. 4), revealed the apparent K_m of 21 ± 4 μM for Ca^{2+} and of 170 ± 30 μM for Mn^{2+}. This observation suggests greater affinity of TMEM165 for Ca^{2+} than for Mn^{2+}, which is consistent with our previously shown data for Gdt1p (4).

Impact of CDG specific mutations on transport activity of TMEM165

To assess the impact of the CDG-specific missense mutations E108G, R126H, R126C, and G304R on the transport activity, these mutations were introduced in $^{\Delta 78}$TMEM165 by site-directed mutagenesis. We first verified that all these mutated forms are well-produced in bacteria (Fig. 5*A*). Interestingly, the G304R mutated variant was detected by Western blotting as a product of higher size when compared with the nonmutated or the other mutated versions of $^{\Delta 78}$TMEM165. Then, using the Fura-2-based functional assay in *L. lactis*, we determined their impact on Ca^{2+} and Mn^{2+} transport capacity (Fig. 5*B*) and on the transport kinetics by estimating the apparent K_m (Table 1). The estimated kinetic parameters indicated that none of the missense mutations modulated the affinity of $^{\Delta 78}$TMEM165 for Mn^{2+}, and only $^{\Delta 78}$TMEM165 with R126C and G304R mutations displayed a reduced affinity for Ca^{2+}. The cells expressing $^{\Delta 78}$TMEM165 with the E108G substitution within the conserved motif displayed significantly lower final fluorescence signal (340/380) after $CaCl_2$ addition, as well as less intense final quenching by $MnCl_2$. This indicates a reduced capacity of the mutated protein to transport Ca^{2+} and Mn^{2+} although no reduced affinity for the two cations. Similarly, a drop (although to a lesser extent) in the Ca^{2+}/Mn^{2+} transport capacity was also observed for $^{\Delta 78}$TMEM165-R126C. Interestingly, the substitution of the same arginine at position 126 to histidine (R126H) resulted in no reduction of the transport capacity for the two cations. No significant reduction of Ca^{2+} or Mn^{2+} transport capacity was observed for the $^{\Delta 78}$TMEM165 containing G304R mutation.

Modulation of yeast cation homeostasis by the mutated forms of TMEM165

To further explore the functional impact of the CDG-associated missense mutations, we performed heterologous expression of the mutated variants of $^{\Delta 78}$TMEM165 back in *S. cerevisiae* and observed the capability to overcome Ca^{2+} and Mn^{2+} stress. As observed in the phenotype complementation assay (Fig. 6*A*), expression of $^{\Delta 78}$TMEM165 carrying R126H or R126C mutations led to only partially decreased growth of the *gdt1Δpmr1Δ* strain in the presence of 400 mM $CaCl_2$, whereas the Ca^{2+} tolerance was totally lost when exposed to higher Ca^{2+} concentration (500 mM). The cells expressing $^{\Delta 78}$TMEM165-E108G exhibited comparable growth with that of the negative control and were completely unable to grow in the presence of higher amounts of $CaCl_2$. This indicates that the mutation of the highly conserved glutamate (E108G) fully abolished the Ca^{2+} tolerance of the *gdt1Δpmr1Δ* strain conferred by the nonmutated $^{\Delta 78}$TMEM165. Similar sensitivity to Ca^{2+} exposure was observed for the *gdt1Δpmr1Δ* strain expressing $^{\Delta 78}$TMEM165-G304R. In contrast to the Ca^{2+}-related phenotypes, expression of any of the mutated forms of $^{\Delta 78}$TMEM165 did not affect the ability of the *gdt1Δpmr1Δ* to grow in the presence of high Mn^{2+} concentrations. To verify that the effects of the mutations indeed reflect activity modulation, we further assessed the subcellular localization (Fig. 6*B*). Immunodetection of the subcellular compartments fractionated on a sucrose gradient showed that $^{\Delta 78}$TMEM165 localizes to the same Golgi-containing fractions as Gdt1p and partly to the ER. The detection of the protein in the ER-corresponding fractions might indicate a partial retention in the ER, which might be a consequence of overexpression. Nevertheless, the growth res-

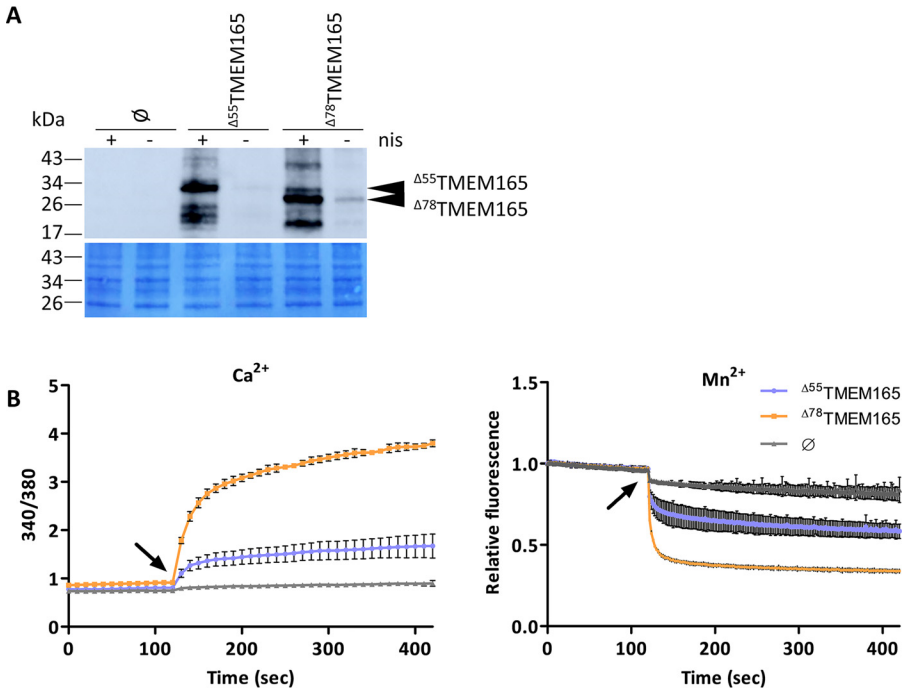

Figure 3. Ca^{2+} and Mn^{2+} transport mediated by truncated TMEM165 expressed in *L. lactis*. *A*, production of the truncated TMEM165 in *L. lactis*. The cells were grown to an A_{600} of 0.5 and incubated in the presence (+*nis*) or not (−*nis*) of nisin (2.5 μg/l) for 2 h to induce the expression of $^{\Delta 55}$TMEM165 or $^{\Delta 78}$TMEM165. The tagged proteins (N terminus) were detected in membrane protein extracts by Western blotting with anti-HA antibodies. ∅, cells with the empty pNZ8048 vector. Coomassie Blue–stained polyvinylidene fluoride membrane was used as loading control. *B*, time-course measurement of the fluorescence emitted by Fura-2 in *L. lactis* DML1 expressing the truncated versions of TMEM165 or containing the empty pNZ8048 vector (∅) in the presence of 75 μM $CaCl_2$ (*left panel*) or 75 μM $MnCl_2$ (*right panel*). The cells were grown to an A_{600} of 0.5, at which the truncated *TMEM165* expression was initiated by addition of 2.5 μg/liter nisin. After a 2-h postinduction time, the cells were washed and incubated for 2 h in the presence of Fura-2/AM. *Left panel*, time-course measurements of the ratio of the fluorescence emitted at 510 nm after excitations at 340 and 380 nm (340/380). *Right panel*, time-course measurements of the quenching by Mn^{2+} of the fluorescence emitted at 510 nm after excitation at 360 nm normalized to the initial fluorescence. $CaCl_2$ or $MnCl_2$ were added after 120 s of measurement (*arrow*), and the *curves* represent the means ($n = 3 \pm$ S.D.).

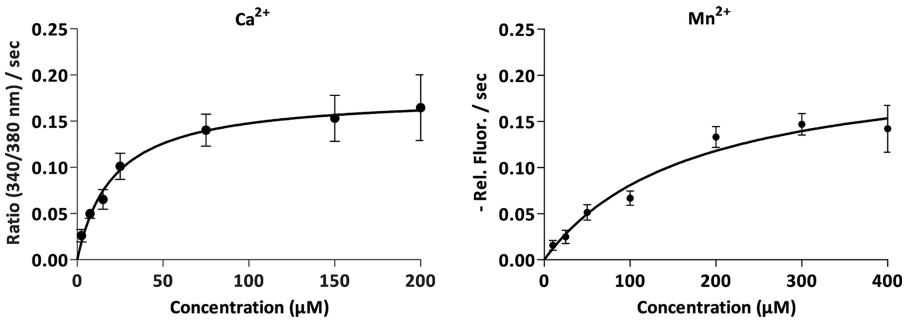

Figure 4. Kinetics of $^{\Delta 78}$TMEM165 assayed by *in vivo* transport measurement in *L. lactis*. The cells were treated as described in the legend to Fig. 3*B*. The Michaelis–Menten *curves* represent the mean initial slopes ($n = 3 \pm$ S.D.) plotted as a function of the free substrate concentration: Ca^{2+} (*left panel*) and Mn^{2+} (*right panel*). The initial slopes were determined from the time-course measurements at various $CaCl_2$ and $MnCl_2$ concentrations. The data were fitted to the Michaelis–Menten equation using GraphPad Prism.

toration of the *gdt1*Δ*pmr1*Δ strain in presence of high Ca^{2+} and Mn^{2+} demonstrates a production of a functional $^{\Delta 78}$TMEM165. The same distribution was also observed for the mutated $^{\Delta 78}$TMEM165 except for $^{\Delta 78}$TMEM165-G304R, which was predominantly detected in the Golgi-containing fractions.

To better understand the observed growth deficiencies, we assessed the glycosylation defects as an indicator of a disturbed cation homeostasis at the Golgi level. Indeed, it has been previously shown that *GDT1*-deficient yeast strain grown at a high external calcium concentrations exhibited protein glycosylation defects (6, 8). In this context, we examined the impact of the CDG-related mutations in the glycosylation process. We assessed by Western blotting differences in migration of the glucanosyltransferase Gas1p, which undergoes *N*- and *O*-linked glycosylation and is often employed as a reporter of Golgi glycosylation capability (8, 13). Compared with the WT strain and in accordance with previously reported data, the *gdt1*Δ*pmr1*Δ strain transformed with an empty vector showed glycosylation defects (Fig. 6*C*). The re-expression of *GDT1* in *gdt1*Δ*pmr1*Δ led to improved glycosylation of Gas1p. The same migration level of Gas1p was also observed for the cells expressing the nonmutated $^{\Delta 78}$TMEM165. Although migration was faster than observed for the WT strain, which might reflect the absence of Pmr1p, the improvement of glycosylation by these two strains indicates that Gdt1p and $^{\Delta 78}$TMEM165 are functional in terms of Golgi-related glycosylation. Similar mobility

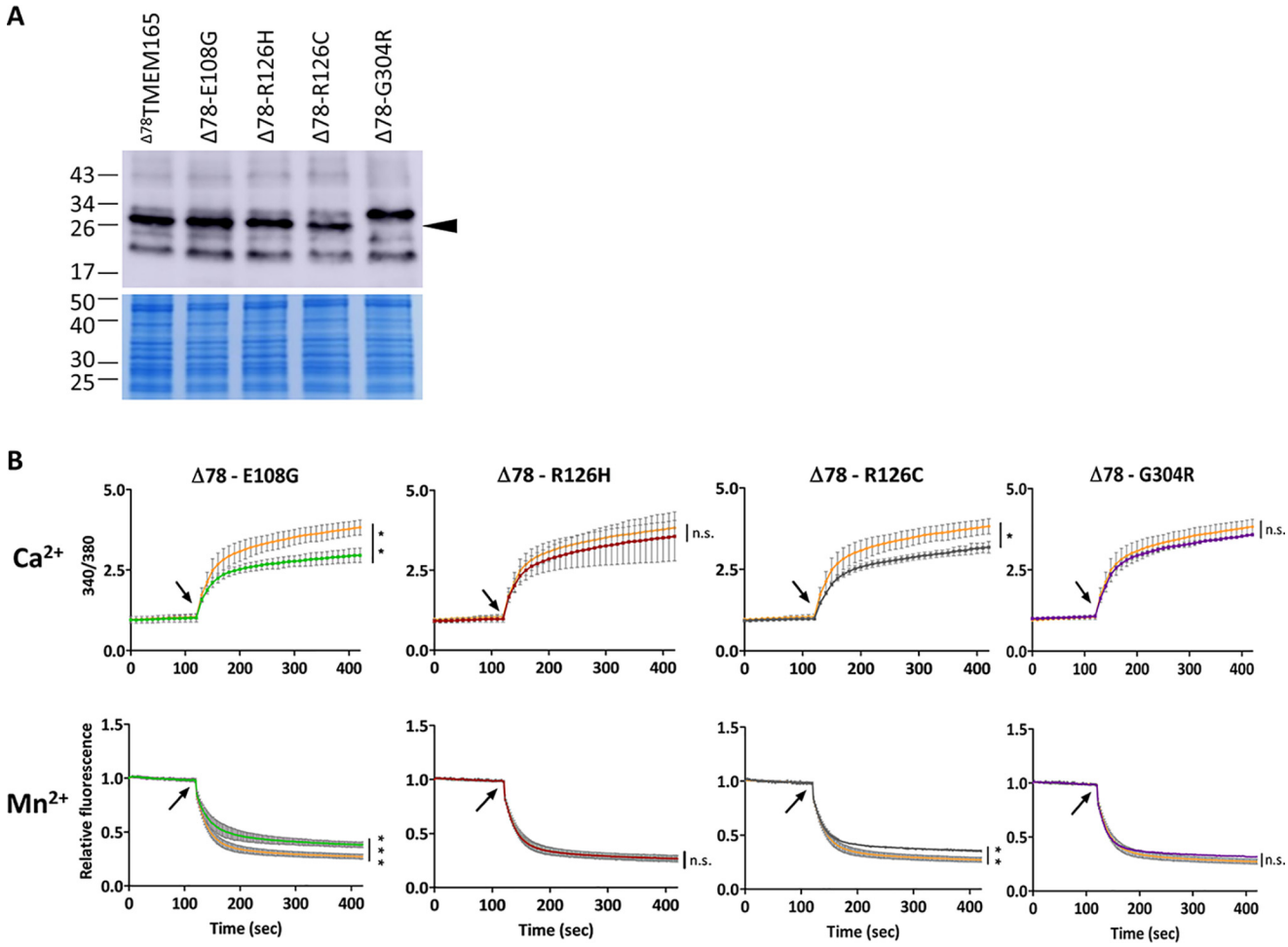

Figure 5. The impact of CDG-related mutations on the transport activity of $^{\Delta 78}$TMEM165 in *L. lactis*. *A*, the HA-tagged proteins (N terminus) were detected in membrane protein extracts by Western blotting with anti-HA antibodies. Colloidal blue–stained gel was used as loading control. *B*, comparison of the fluorescence emitted during time by Fura-2 in *L. lactis* DML1 expressing the nonmutated $^{\Delta 78}$TMEM165 truncated versions (*orange curves*) or $^{\Delta 78}$TMEM165 containing the CDG-related mutations (indicated on the *top* of the graphs). The cells were treated as described in Fig. 3*B*. *Upper panels*, time-course measurements of the ratio of the fluorescence emitted at 510 nm after excitations at 340 and 380 nm (340/380). *Lower panels*, time-course measurements of the quenching by Mn^{2+} of the fluorescence emitted at 510 nm after excitation at 360 nm normalized to the initial fluorescence. $CaCl_2$ (25 μM) or $MnCl_2$ (25 μM) were added after 120 s of measurement (*arrow*), and the curves are represented as means ($n = 3 \pm$ S.D.). The values recorded 5 min after $CaCl_2$ or $MnCl_2$ addition were analyzed by unpaired *t* test. *, $p < 0.05$; **, $p < 0.01$; ***, $p < 0.001$; *ns,* not significant.

Table 1

The apparent K_m (μM) for Ca^{2+} and Mn^{2+} estimated by *in vivo* transport measurements in *L. lactis* expressing the nonmutated $^{\Delta 78}$TMEM165 or $^{\Delta 78}$TMEM165 containing CDG-related mutations

The data are represented as means ± S.D. ($n = 3$).

	$^{\Delta 78}$TMEM165	Δ78-E108G	Δ78-R126H	Δ78-R126C	Δ78-G304R
Ca^{2+}	20.9 ± 4.1	21.4 ± 3.5[a]	19.8 ± 2.7[a]	40.8 ± 9.7[b]	35.3 ± 4.6[b]
Mn^{2+}	170 ± 30	155 ± 35[a]	179 ± 50[a]	221 ± 66[a]	157 ± 42[a]

[a] Not significant.
[b] $p < 0.05$ (unpaired *t* test).

of Gas1p was observed for the strains expressing the mutated $^{\Delta 78}$TMEM165-R126H and $^{\Delta 78}$TMEM165-R126C, whereas the strains producing $^{\Delta 78}$TMEM165-E108G and $^{\Delta 78}$TMEM165-G304R showed glycosylation defects. This observation correlates well with the defective growth of the corresponding mutants at high Ca^{2+} concentrations.

Because all the forms were well-produced, the aforementioned deficiencies are not due to protein abundance. It rather indicates a disturbed cation homeostasis at the Golgi level probably arising from the impaired activity of the two mutated variants of $^{\Delta 78}$TMEM165. Interestingly, the $^{\Delta 78}$TMEM165-G304R mutated form was detected as a product of higher size when compared with the other $^{\Delta 78}$TMEM165 forms, as previously observed when the proteins are expressed in *L. lactis* (Figs. 5*A* and 6*D*).

Discussion

Heterologous expression of human proteins in unicellular models has become a valuable strategy for their characterization. In this study, we succeeded in the heterologous production of functional human TMEM165 protein in yeast and bacterial hosts. This allowed us to provide for the first time direct

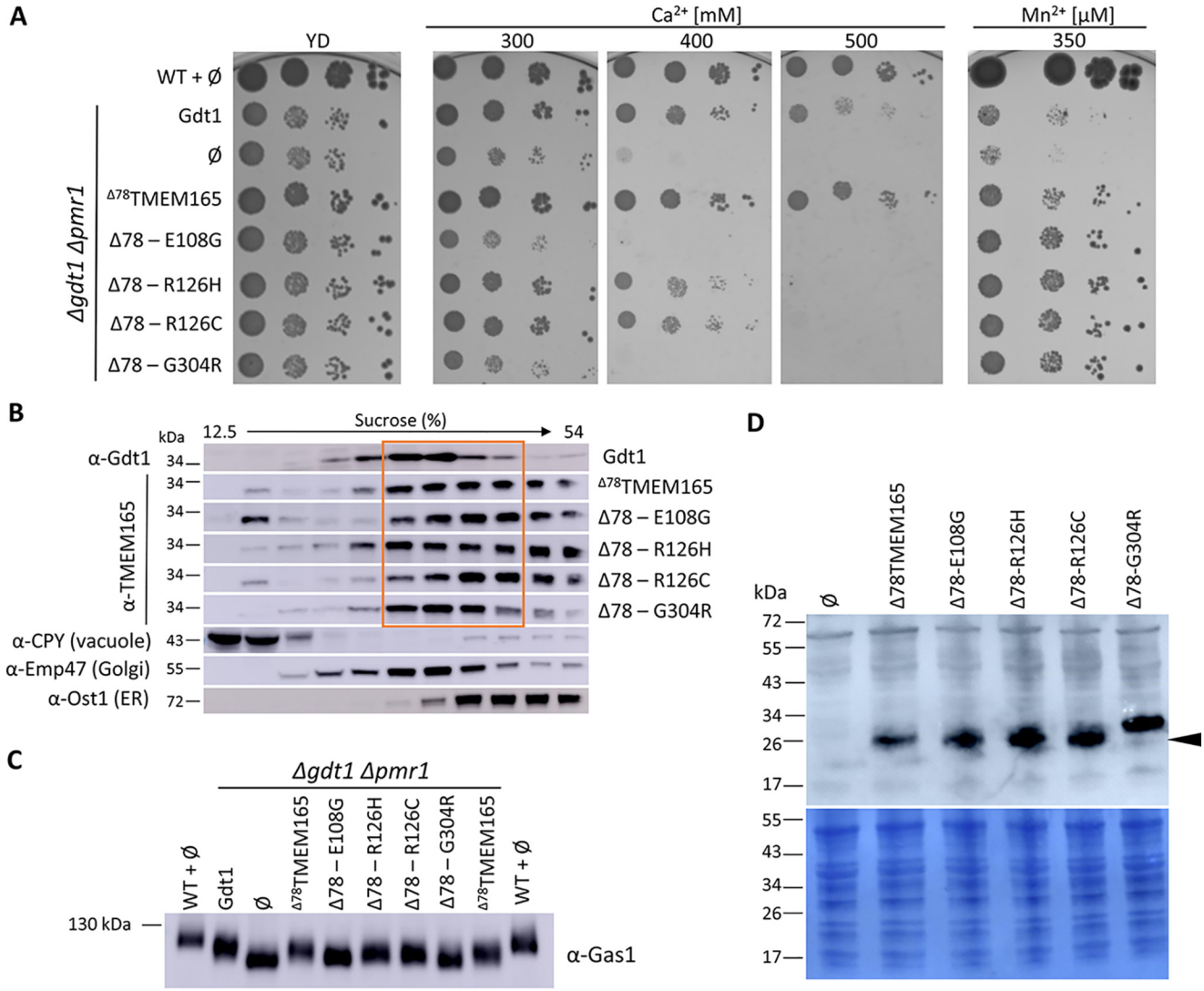

Figure 6. *A*, phenotypic effects of $^{\Delta 78}$TMEM165-CDG-related mutations within *gdt1*Δ*pmr1*Δ strain. The *gdt1*Δ*pmr1*Δ strain expressed *GDT1*, $^{\Delta 78}$TMEM165 truncated version, or $^{\Delta 78}$TMEM165 containing CDG-causing mutations. ∅, *gdt1*Δ*pmr1*Δ with the empty pRS416 vector. The cells were treated as described in the legend to Fig. 1*B*. *B*, subcellular fractionation of *gdt1*Δ*pmr1*Δ strain expressing *GDT1*, $^{\Delta 78}$TMEM165, or mutated $^{\Delta 78}$TMEM165. Each strain was lysed and fractionated on a sucrose gradient. The collected fractions were analyzed by Western blotting using antibodies against Gdt1 or TMEM165 and against markers of the different subcellular compartments (CPY, Emp47, and Ost1). The distributions of the organellar markers shown here are representatives of those observed in all the strains. *C*, glycosylation of Gas1p. Total membrane proteins were extracted from the WT strain or *gdtl*Δ*pmr1*Δ strains expressing *GDT1*, $^{\Delta 78}$TMEM165 truncated version, or $^{\Delta 78}$TMEM165 containing CDG-causing mutations. The cells were grown in MD-U supplemented with 200 mM $CaCl_2$ to an A_{600} of 3. The levels of Gas1p were analyzed by Western blotting with anti-Gas1 antibodies. *D*, production of the different TMEM165 versions in *gdtl*Δ*pmr1*Δ strain. Total protein extracts of cells grown in MD-U medium to an A_{600} of 3 were analyzed by Western blotting with antibodies directed against TMEM165.

biochemical evidence for the calcium and manganese transport of this CDG-related protein and to investigate the impact of disease-causing mutations on the transport activity.

We used codon optimization and genetic engineering of TMEM165 to optimize expression level and activity in yeast and bacteria. Indeed, codon optimization radically improved protein production in *S. cerevisiae*, and deletion of the first residues of TMEM165 significantly increased its activity in yeast and bacteria. A similar effect of the N-terminal truncation on Ca^{2+} tolerance was also observed for BICAT2, one of the *Arabidopsis thaliana* UPF0016 members, when expressed in yeast (14). This strengthens the fact that the UPF0016 N-terminal region, which shows the highest variability and which has been predicted to be cleavable secretory pathway signal peptide for some members, needs to be at least partly removed for optimal heterologous production of functional eukaryotic UPF0016 members. This also suggests, as previously stated by Demaegd *et al.* (2) and Schneider *et al.* (15), that this N-terminal region could participate in regulation of the cation homeostasis as an autoinhibitory/regulatory domain. In our study, we show that production of this codon-optimized truncated version of TMEM165 modulates yeast resistance to high external Mn^{2+} concentrations, cellular Mn^{2+} accumulation, and glycosylation efficiency, all reflecting an effect on the homeostasis of manganese in this host. To further investigate whether TMEM165 transports cations, we took advantage of the use of $^{\Delta 78}$TMEM165-producing *L. lactis* cells loaded with the fluorescent probe Fura-2. This bacterium has been shown to be valuable expression system because of targeting the expressed membrane proteins in functional form to the cytoplasmic membrane, without

the formation of inclusion bodies (16). With this system, we confirmed the previously suggested Ca^{2+} transport activity (3) and showed for the first time direct Mn^{2+} transport by this human protein. This suggests that the effect of TMEM165 on manganese homeostasis previously observed in human cells (affected stability of the Mn^{2+}-sensitive protein GPP130, Mn^{2+}-induced degradation of TMEM165, and restoration of the TMEM165-induced glycosylation defects by Mn^{2+} (5, 7)) could indeed be related to its Mn^{2+} transport ability at the Golgi. In addition, this further reinforces the involvement of the UPF0016 members in manganese homeostasis that was previously shown for bacterial, plant, yeast, and human members and their subsequent connection to essential cellular processes like photosynthesis and glycosylation. Confirmation of the transport activity of TMEM165 directly in human cells will be required in the future.

Missense mutations were recently identified in TMEM165 in patients with CDGs. In this study, we took advantage of the development of the $^{\Delta 78}$TMEM165-producing yeast and bacterial cells to investigate the impact of the identified missense mutations on the transport activity. Introduction of the mutation E108G within the conserved UPF0016 motif of TMEM165 led to reduced Ca^{2+} and Mn^{2+} transport activity, both in bacteria and in yeast. In contrast, TMEM165 with mutation R126H seems to be the least affected in terms of the transport activity, only showing impaired yeast growth at the highest tested Ca^{2+} concentration. The mutations R126C and G304R showed intermediate results, their transport ability being impaired only in bacteria or in yeast, respectively. In fact, R126H/C missense mutations have been previously shown to affect the subcellular localization of TMEM165 in HeLa cells, being predominantly detected in lysosomes (10). Additionally, complementation assay in yeast showed that the equivalent mutations (R71H and R71C) introduced in Gdt1p had no effect on the protein function (10), which further supports the hypothesis that the disease caused by TMEM165 with R126H/C mutations can be linked to altered protein localization in human cells rather than its transport activity. The TMEM165-G304R is also reported as mislocalized compared with the WT protein (10). In addition, Western blotting analysis revealed altered protein size that could arise from mutation-induced alteration of post-translational protein modifications. In this context, the molecular causes of the pathogenicity of this mutation remain unclear. In contrast, the TMEM165-E108G was found correctly localized in HeLa cells and only slightly restores the glycosylation defects observed in TMEM165-knockdown cells (5, 17). Combined with our results, this suggests that the mutation of the highly conserved Glu^{108} causes glycosylation defects through impaired cation transport activity of the protein.

No matter whether resulting in altered localization or transport activity, the presence of specific mutations within TMEM165 might alter cation homeostasis at the Golgi level where protein maturation takes place. Another type of CDG, related to the presence of specific mutations within the cell-surface Mn^{2+} importer SLC39A8, was similarly linked to protein undergalactosylation because of altered cellular manganese homeostasis (18). These two examples clearly illustrate the key importance of proper cation regulation at the Golgi for essential processes like glycosylation. At present, it remains an important issue to distinguish whether defective cytosolic or Golgi concentrations of Ca^{2+} and/or Mn^{2+} are responsible for the TMEM165-CDGs, these two cations being important for proper glycosylation by modulating intracellular trafficking within the secretory pathway, influencing protein stability, or acting as cofactors. Identification of TMEM165 selectivity mutants transporting only Ca^{2+} or Mn^{2+} might help answering this question in the future.

Experimental procedures

Strains and culture media

The *S. cerevisiae* strains used in this study were BY4741 (*Mata his3Δ1 leu2Δ0 met15Δ0 ura3Δ0*, Euroscarf) and BY *gdt1Δ pmr1Δ* (*Matα his3Δ1 leu2Δ0 ura3Δ0 met15Δ0 gdt1*::*KanMX4 pmr1*::*KanMX4*) (3). Nontransformed yeast cells were routinely cultured at 28 °C in YD medium (2% yeast extract KAT, 2% glucose) under agitation. Cells transformed with plasmids were grown in MD-U minimal medium (0.2% yeast nitrogen base without amino acids and ammonium sulfate (Difco), 76 mM NH_4Cl, 2% glucose, supplemented with 1.92 g/liter of Drop-Out mixture without Uracil (Formedium, UK)). Solid media were produced by addition of 2% agar to the mixture. The *L. lactis* DML1 strain was kindly provided by B. Poolman (Groningen, The Netherlands). *L. lactis* cells were grown in M17 broth according to Terzaghi (Merck Millipore) supplemented with 1% glucose at 28 °C. Cells transformed with the pNZ8048 plasmid were grown in the presence of 10 μg/ml chloramphenicol. Expression of genes under the control of the pNisA promoter was induced by 2.5 μg/lite nisin at the log phase (A_{600} = ~0.4–0.5).

Vector construction

Yeast and bacterial plasmids were obtained following standard molecular biology protocols, and the authenticity of all genetic constructs was validated by sequencing. The yeast plasmids pRS416-pTPI-GDT1 (overexpressing *GDT1* under the control of *TPI1*, triose-phosphate isomerase, constitutive promoter), pRS416-pTPI-TMEM165, and pRS416-pTPI-$^{\Delta 55}$TMEM165 (overexpressing codon nonoptimized TMEM165 and $^{\Delta 55}$TMEM165) were obtained previously (3). The full-length TMEM165 gene was codon-optimized for the *S. cerevisiae* expression system (Fig. S1) and chemically synthesized (GeneScript). The codon-optimized truncated $^{\Delta 55}$TMEM165 and $^{\Delta 78}$TMEM165 were obtained by amplification from the codon-optimized full-length gene. The DNA fragments were digested with XbaI/XhoI and integrated in the pRS416-pTPI plasmid. For the heterologous expression in *L. lactis*, we used pNZ8048 plasmid expressing 10HIS-HA-TEV-tagged (N-terminal) $^{\Delta 55}$TMEM165 or $^{\Delta 78}$TMEM165 truncated version under the control of the nisin-inducible promoter. The nucleotide sequences were codon-optimized for bacterial expression (MeKaGene) (Fig. S2), chemically synthesized (Integrated DNA Technologies), digested with NcoI/HindIII, and cloned into the pNZ8048 vector. The TMEM165-CDG mutations were inserted in the codon-optimized $^{\Delta 78}$TMEM165 by triple PCR using overlapping primers containing the desired nucleotide changes (19). The primers used to insert the point mutants are

Table 2
Primers used for the site-directed mutagenesis
The underlined letters indicate the changes in nucleotide sequence. The bold letters indicate restriction sites.

Name	Sequence 5′ → 3′
Insertion into pRS416-pTPI	
pRS-78TMEM-Fa	GTA**TCTAGA**ATGCATACTAACAAAGA **(XbaI)**
pRS-TMEM-Ra2	CAT**CTCGAG**TTAAAAACCTG **(XhoI)**
pRS-E108G-F	TATTGTATCTGGACTTGGAG
pRS-E108G-R	CTCCAAGTCCAGATACAATA
pRS-R126H-F	GATATAATCATTTGACAGTTCTTG
pRS-R126H-R	CAAGAACTGTCAAATGATTATATC
pRS-R126C-F	GATATAATTGTTTGACAGTTCTTG
pRS-R126C-R	CAAGAACTGTCAAACAATTATATC
pRS-G304R-F	GTAACCATTATTAGAGGAATTG
pRS-G304R-R	CAATTCCTCTAATAATGGTTAC
Insertion into pNZ8048	
Ins-F-4	AGCTCAG**CCATGG**GTCATC **(NcoI)**
Ins-R-1	CTCTTACCTTG**AAGCTT**TCA **(HindIII)**
E108G-F	TATTGTGTCCGGATTAGGTG
E108G-R	CACCTAATCCGGACACAATA
R126H-F	CTATAACCACCTGACCGTG
R126H-R	CACGGTCAGGTGGTTATAGC
R126C-F	CTATAACTGCCTGACCGTG
R126C-R	CACGGTCAGGCAGTTATAGC
G304R-F	ACCATCATTAGAGGAATCG
G304R-R	CGATTCCTCTAATGATGGTGAC

listed in Table 2. DNA amplification was carried out with the Phusion polymerase (New England Biology). The amplified PCR products for *S. cerevisiae* expression system were digested with XbaI/XhoI and integrated into the pRS416-pTPI plasmid. The PCR products for *L. lactis* expression system were digested with NcoI/HindIII and cloned into the pNZ8048 vector. Yeast transformation was performed in triplicate following the method of Gietz *et al.* (20). *L. lactis* transformation was performed in triplicate by electroporation as described by Holo *et al.* (21).

In vivo transport assay

The *in vivo* transport measurements were carried out using the fluorescent dye Fura-2/AM as described previously (4). In short, *L. lactis* DML1 cells transformed with the empty or pNZ8048 plasmid harboring the different versions of TMEM165 were grown in M17 broth. At an A_{600} of 0.5, induction was initiated by adding 2.5 μg/liter nisin in the extracellular medium. After a postinduction time of 2 h, the cells were harvested (3,000 × *g* for 7 min) and washed twice with the washing buffer (50 mM Tris-HCl, pH 7.4, 100 mM KCl, and 1 mM $MgCl_2$). The washed cells were resuspended in the same buffer supplemented with 0.2 mM EDTA (pH 8.0) and incubated for 10 min. The harvested cells were then incubated with the washing buffer supplemented with 10 μM Fura-2/AM (Molecular Probes) and 1.7 mM probenecid for 2 h at 28 °C under agitation. The cells were subsequently washed three times in the presence of 1 mM EGTA, and the final pellet was resuspended in 10 ml of the washing buffer supplemented with 1.7 mM probenecid. Prior to measurements, this latter solution was treated with calcium sponges (BAPTA chelator coupled to a polymer matrix, Invitrogen). The signal was recorded either with a single excitation wavelength of 360 nm (quenching measurements) or with two excitation wavelengths of 340 and 380 nm (ratiometric measurements), the emission wavelength being set at 510 nm. $MnCl_2$ or $CaCl_2$ were added in the extracellular medium at the indicated concentrations. The data were recorded using JASCO FP8500 fluorimeter controlled by the Spectra Manager software. The transport kinetics of $^{\Delta 78}$TMEM165 were analyzed at Ca^{2+} and Mn^{2+} concentrations ranging from 2.5 to 200 μM $CaCl_2$ and 10 to 400 μM $MnCl_2$, and the determination of the apparent K_m was performed as described previously (4).

ICP-AES analysis

For determination of the total intracellular Mn^{2+} content, the yeast transformants were grown in MD-U medium to an A_{600} of 3. The cells were then collected by vacuum filtration using membrane filters (Millipore, 0.45-μm pore size) and washed twice with 2 ml of 1 mM EGTA (pH 8) and twice with 2 ml of H_2O. The cells were collected in heat-resistant beakers in 10 ml of H_2O and dried at 95 °C overnight and then in a desiccator for 24 h. The dry matter was mineralized by heating at 500 °C overnight. The ashed sample was subsequently dissolved in 10 ml of 6.5% HNO_3 for analysis on an ICAP 6500 spectrometer (Thermo Scientific).

Subcellular fractionation

Subcellular compartments were fractionated on a discontinuous sucrose gradient ranging from 12.5 to 54% as described previously (3). The fractions were separated by SDS-PAGE and analyzed by immunoblotting. Detection of Emp47, Ost1, and CPY was used as Golgi, ER, and vacuolar markers, respectively.

Western blotting

Total protein extracts from yeast cells were prepared as follows. The cells grown in the indicated media to A_{600} of 3 were harvested by centrifugation at 3,000 × *g* for 5 min, washed with cold water, and resuspended in 200 μl of lysis buffer (250 mM sorbitol, 50 mM imidazole, 1 mM $MgCl_2 \cdot 6H_2O$, pH 7.5) containing phenylmethylsulfonyl fluoride at a final concentration of 1 mM and 0.1% protease inhibitor mixture (Roche). The cells were lysed with glass beads by vortexing (eight 30-s pulses followed by 15-s pauses on ice). Cell debris and unbroken cells were eliminated by centrifugation at 3,000 × *g* at 4 °C for 20 s. The total membrane fractions from *L. lactis* were prepared as described earlier (8), except that the cells were not incubated 30 min at 28 °C before the lysis with glass beads. The protein concentrations were determined using the bicinchoninic acid assay according to Smith *et al.* (22). Aliquots (30 μg) of protein extracts were mixed with sample loading buffer (80 mM Tris-HCl, pH 6.8, 2% SDS, 10% glycerol, 0.005% bromphenol blue, 1% DTT), separated by SDS-PAGE using 4–15% Mini-PROTEAN TGX gels (Bio-Rad), and transferred using the Trans-Blot turbo transfer system (Bio-Rad). To detect Gdt1p the extracts were separated on a 10% handmade SDS-PAGE gel and transferred to a polyvinyl difluoride membrane (Millipore) using a semidry transfer system (Bio-Rad) in 50 mM Tris, 40 mM glycine, 1.3 mM SDS, 20% methanol. Primary antibodies used in this study were rabbit anti-TMEM165 (1:2,000 dilution; Proteintech), rabbit anti-Gdt1 (1:333 dilution; (3)), rat anti-hemagglutinin (anti-HA; 1:1,000 dilution; Roche), rabbit anti-Ost1 (1:2,000 dilution; gift from R. Gilmore), rabbit anti-Emp47, rabbit anti-CPY, and rabbit anti-Gas1 (all 1:2,000 dilution; gifts from H. Riezman, Geneva, Switzerland). Incubation with primary antibodies was followed by incubation with horseradish

peroxidase–coupled anti-rat (1:10,000 dilution; Thermo Scientific) or anti-rabbit (1:10,000 dilution; IMEX) IgG antibodies. Bound antibodies were revealed using Lumi-Light Western blotting substrate (Roche Diagnostics), and the emitted light was captured with Amersham Biosciences Imager 600 (GE Healthcare Bio-Sciences AB). The Western analyses were performed from at least three biological replicates.

Yeast calcium and manganese sensitivity assays

For drop tests, the yeast cells were precultured overnight in 5 ml of MD-U medium. Each culture was then adjusted to an A_{600} of 0.3. Aliquots of 4 μl of the adjusted culture and of 10-fold serial dilutions were spotted on solid YD media or MD-U media containing the indicated concentrations of $CaCl_2$ or $MnCl_2$. The plates were incubated and monitored for 3–5 days at 28 °C.

Author contributions—J. S., L. T., A. D., P. G., and P. M. conceptualization; J. S. investigation; J. S. methodology; J. S. writing-original draft; J. S. and P. M. writing-review and editing; L. T. and A. D. visualization; P. G. software; P. M. supervision; P. M. funding acquisition.

Acknowledgments—We thank B. Poolman for providing the DML1 strain and A. Iserentant for technical assistance with the ICP-AES measurements in yeast.

References

1. Foulquier, F., Amyere, M., Jaeken, J., Zeevaert, R., Schollen, E., Race, V., Bammens, R., Morelle, W., Rosnoblet, C., Legrand, D., Demaegd, D., Buist, N., Cheillan, D., Guffon, N., Morsomme, P., *et al.* (2012) TMEM165 deficiency causes a congenital disorder of glycosylation. *Am. J. Hum. Genet.* **91,** 15–26 CrossRef Medline
2. Demaegd, D., Colinet, A. S., Deschamps, A., and Morsomme, P. (2014) Molecular evolution of a novel family of putative calcium transporters. *PLoS One* **9,** e100851 CrossRef Medline
3. Demaegd, D., Foulquier, F., Colinet, A. S., Gremillon, L., Legrand, D., Mariot, P., Peiter, E., Van Schaftingen, E., Matthijs, G., and Morsomme, P. (2013) Newly characterized Golgi-localized family of proteins is involved in calcium and pH homeostasis in yeast and human cells. *Proc. Natl. Acad. Sci. U.S.A.* **110,** 6859–6864 CrossRef Medline
4. Thines, L., Deschamps, A., Sengottaiyan, P., Savel, O., Stribny, J., and Morsomme, P. (2018) The yeast protein Gdt1p transports Mn^{2+} ions and thereby regulates manganese homeostasis in the Golgi. *J. Biol. Chem.* **293,** 8048–8055 CrossRef Medline
5. Potelle, S., Dulary, E., Climer, L., Duvet, S., Morelle, W., Vicogne, D., Lebredonchel, E., Houdou, M., Spriet, C., Krzewinski-Recchi, M. A., Peanne, R., Klein, A., de Bettignies, G., Morsomme, P., Matthijs, G., *et al.* (2017) Manganese-induced turnover of TMEM165. *Biochem. J.* **474,** 1481–1493 CrossRef Medline
6. Dulary, E., Yu, S. Y., Houdou, M., de Bettignies, G., Decool, V., Potelle, S., Duvet, S., Krzewinski-Recchi, M. A., Garat, A., Matthijs, G., Guerardel, Y., and Foulquier, F. (2018) Investigating the function of Gdt1p in yeast Golgi glycosylation. *Biochim. Biophys. Acta Gen. Subj.* **1862,** 394–402 CrossRef Medline
7. Potelle, S., Morelle, W., Dulary, E., Duvet, S., Vicogne, D., Spriet, C., Krzewinski-Recchi, M. A., Morsomme, P., Jaeken, J., Matthijs, G., De Bettignies, G., and Foulquier, F. (2016) Glycosylation abnormalities in Gdt1p/TMEM165 deficient cells result from a defect in Golgi manganese homeostasis. *Hum. Mol. Genet.* **25,** 1489–1500 CrossRef Medline
8. Colinet, A. S., Sengottaiyan, P., Deschamps, A., Colsoul, M. L., Thines, L., Demaegd, D., Duchêne, M. C., Foulquier, F., Hols, P., and Morsomme, P. (2016) Yeast Gdt1 is a Golgi-localized calcium transporter required for stress-induced calcium signaling and protein glycosylation. *Sci. Rep.* **6,** 24282 CrossRef Medline
9. Schulte Althoff, S., Grüneberg, M., Reunert, J., Park, J. H., Rust, S., Mühlhausen, C., Wada, Y., Santer, R., and Marquardt, T. (2016) TMEM165 deficiency: postnatal changes in glycosylation. *JIMD Reports* **26,** 21–29 Medline
10. Rosnoblet, C., Legrand, D., Demaegd, D., Hacine-Gherbi, H., de Bettignies, G., Bammens, R., Borrego, C., Duvet, S., Morsomme, P., Matthijs, G., and Foulquier, F. (2013) Impact of disease-causing mutations on TMEM165 subcellular localization, a recently identified protein involved in CDG-II. *Hum. Mol. Genet.* **22,** 2914–2928 CrossRef Medline
11. Colinet, A. S., Thines, L., Deschamps, A., Flemal, G., Demaegd, D., and Morsomme, P. (2017) Acidic and uncharged polar residues in the consensus motifs of the yeast Ca2+ transporter Gdt1p are required for calcium transport. *Cell. Microbiol.* **19,** 12729 CrossRef Medline
12. Rudolph, H. K., Antebi, A., Fink, G. R., Buckley, C. M., Dorman, T. E., LeVitre, J., Davidow, L. S., Mao, J. I., and Moir, D. T. (1989) The yeast secretory pathway is perturbed by mutations in PMR1, a member of a Ca^{2+} ATPase family. *Cell* **58,** 133–145 CrossRef Medline
13. Gentzsch, M., and Tanner, W. (1997) Protein-*O*-glycosylation in yeast: protein-specific mannosyltransferases. *Glycobiology* **7,** 481–486 CrossRef Medline
14. Frank, J., Happeck, R., Meier, B., Hoang, M. T. T., Stribny, J., Hause, G., Ding, H., Morsomme, P., Baginsky, S., and Peiter, E. (2019) Chloroplast-localized BICAT proteins shape stromal calcium signals and are required for efficient photosynthesis. *New Phytol.*. **221,** 866–880 CrossRef Medline
15. Schneider, A., Steinberger, I., Herdean, A., Gandini, C., Eisenhut, M., Kurz, S., Morper, A., Hoecker, N., Rühle, T., Labs, M., Flügge, U. I., Geimer, S., Schmidt, S. B., Husted, S., Weber, A. P., *et al.* (2016) The evolutionarily conserved protein photosynthesis affected mutant 71 is required for efficient manganese uptake at the thylakoid membrane in *Arabidopsis*. *Plant Cell* **28,** 892–910 Medline
16. Kunji, E. R., Slotboom, D. J., and Poolman, B. (2003) *Lactococcus lactis* as host for overproduction of functional membrane proteins. *Biochim. Biophys. Acta* **1610,** 97–108 CrossRef Medline
17. Lebredonchel, E., Houdou, M., Potelle, S., de Bettignies, G., Schulz, C., Krzewinski Recchi, M. A., Lupashin, V., Legrand, D., Klein, A., and Foulquier, F. (2019) Dissection of TMEM165 function in Golgi glycosylation and its Mn^{2+} sensitivity. *Biochimie* **165,** 123–130 CrossRef Medline
18. Park, J. H., Hogrebe, M., Grüneberg, M., DuChesne, I., von der Heiden, A. L., Reunert, J., Schlingmann, K. P., Boycott, K. M., Beaulieu, C. L., Mhanni, A. A., Innes, A. M., Hörtnagel, K., Biskup, S., Gleixner, E. M., Kurlemann, G., *et al.* (2015) SLC39A8 deficiency: a disorder of manganese transport and glycosylation. *Am. J. Hum. Genet.* **97,** 894–903 CrossRef Medline
19. Ho, S. N., Hunt, H. D., Horton, R. M., Pullen, J. K., and Pease, L. R. (1989) Site-directed mutagenesis by overlap extension using the polymerase chain reaction. *Gene* **77,** 51–59 CrossRef Medline
20. Gietz, D., St Jean, A., Woods, R. A., and Schiestl, R. H. (1992) Improved method for high efficiency transformation of intact yeast cells. *Nucleic Acids Res.* **20,** 1425 CrossRef Medline
21. Holo, H., and Nes, I. F. (1989) High-frequency transformation, by electroporation, of *Lactococcus lactis* subsp. cremoris grown with glycine in osmotically stabilized media. *Appl. Environ. Microbiol.* **55,** 3119–3123 CrossRef Medline
22. Smith, P. K., Krohn, R. I., Hermanson, G. T., Mallia, A. K., Gartner, F. H., Provenzano, M. D., Fujimoto, E. K., Goeke, N. M., Olson, B. J., and Klenk, D. C. (1985) Measurement of protein using bicinchoninic acid. *Anal. Biochem.* **150,** 76–85 CrossRef Medline